J Mol Cell Cardiol **32**, 247–259 (2000)
doi:10.1006/jmcc.1999.1069, available online at http://www.idealibrary.com on IDEAL®

Sarcomere Length–tension Relationship of Rat Cardiac Myocytes at Lengths Greater than Optimum

Wieland K. K. Weiwad[1], Wolfgang A. Linke*[2] and Manfred H. P. Wussling[1]

[1]*Julius Bernstein Institute of Physiology, Martin Luther University Halle-Wittenberg, D-06097 Halle, Germany, and* [2]*Institute of Physiology II, University of Heidelberg, Im Neuenheimer Feld 326, D-69120 Heidelberg, Germany*

(Received 13 August 1999, accepted in revised form 15 November 1999)

W. K. K. Weiwad, W. A. Linke and M. H. P. Wussling. Sarcomere Length–tension Relationship of Rat Cardiac Myocytes at Lengths Greater than Optimum. *Journal of Molecular and Cellular Cardiology* (2000) **32**, 247–259. The study was aimed at determining both passive and Ca^{2+}-activated forces of single skinned rat cardiac cells. Particular attention was paid to the descending limb of the active length–tension curve while the sarcomeric order of stretched cells was investigated before and during contraction. To analyse sarcomere length and sarcomere-length inhomogeneity, a fast Fourier transform (FFT) was employed. The fundamental frequency in the FFT spectrum is a measure of sarcomere length. The full-width-half-maximum of the first-order line is a measure of sarcomere-length inhomogeneity. In relaxing buffer, the sarcomere-length inhomogeneity of skinned cells increased linearly with mean sarcomere length. Upon Ca^{2+}-dependent activation of skinned cells contracting isometrically, mean sarcomere length decreased slightly and inhomogeneity increased; both effects were greater at higher Ca^{2+} concentrations. Maximum activation was reached at sarcomere lengths between 2.2 and 2.4 μm, whereas the descending limb of the active length–tension curve approached zero force already at $\sim$2.8 μm. This steep force decline could not be explained by overly inhomogeneous sarcomere lengths in very long, contracting cells. Rather, the results of mechanical measurements on single cardiac myofibrils implied that high stretching is accompanied by irreversible structural alterations within cardiac sarcomeres, most likely thick-filament disarray and disruption of binding sites between myosin and titin due to changes in titin's tertiary structure. Loss of a regular thick-filament organization may then impair active force generation. We conclude that the descending limb of the cardiac length–tension curve is determined both by the degree of actin–myosin overlap and by the intrinsic properties of titin filaments.

Key Words: Cardiac muscle mechanics; Fourier transform; Active tension; Passive tension; Titin; Connectin.

Introduction

The mechanical properties of cardiac-muscle preparations have been extensively studied for several decades (for reviews, see Allen and Kentish[1] and Brady[2]). The forces developed under both relaxing and activating conditions have been investigated in multicellular specimens, single cardiac myocytes, and isolated single myofibrils. Progress has been made in recent years towards an understanding of the origin of passive tension in non-activated muscle.[3,4] Activated cardiac muscle exhibits a typical sarcomere-length (SL) dependence of force development with a relatively steep force rise between 1.7 and 2.2–2.3 μm SL, particularly at intermediate Ca^{2+} activation levels,[5–9] which explains the enhanced contractility of the heart after increased diastolic filling (Frank–Starling mechanism). The SL-active tension curve is less well defined at lengths greater than optimum, essentially because it is difficult to pull conventional cardiac preparations such as papillary muscles or trabeculae to beyond

* Please address all correspondence to: W. A. Linke.

0022–2828/00/020247+13 $35.00/0

2.4 μm SL. Efforts have been made to determine the full-range SL–tension curve of rat and dog cardiac myocytes,[10] but the sarcomeres could not be stretched to the point where active tension development was zero. Nevertheless, in many textbooks it is tacitly assumed that the descending limb of the SL–tension relation of cardiac muscle is basically similar to that of skeletal muscle. Accordingly, active force is thought to drop to zero at 3.6–3.9 μm SL,[11] i.e. at the end of overlap between actin and myosin filaments. A main goal of this study was to investigate whether this scenario is indeed correct.

Passive and active forces of single rat cardiomyocytes were measured over a wide range of lengths. Passive tension was also investigated in isolated single cardiac myofibrils. A computer-aided method was employed to determine SL and SL inhomogeneity from the intensity profiles recorded in selected regions along a myocyte.[12,13] The analysis technique is based on the fast Fourier transform (FFT).[14,15] Mean SL is obtained by measuring and inverting the fundamental frequency of the FFT spectrum. The full width at half maximum (FWHM) of the first-order peak is a measure of SL inhomogeneity. The focus of this study was the descending limb of the active length–tension curve. We found that rat cardiac myocytes exhibit a relatively short descending limb, which cannot be explained by increased SL inhomogeneity of highly stretched, contracting sarcomeres. Instead, mechanical analysis of the elastic properties of titin filaments in cardiac sarcomeres strongly suggests an involvement of these filaments in the determination of the abbreviated descending limb.

Materials and Methods

Experimental setup and force measurement

The experimental apparatus (Fig. 1A) is centered around a Nikon Diaphot-TMD inverted microscope, with micromanipulators mounted on each side. One manipulator holds a fine glass needle, the other a force transducer (403A, Cambridge Technologies Inc.), to which a fine wire is attached. Skinned rat cardiac myocytes were glued between the tips of the wire and the glass needle (Fig. 1B). The image of a cell was monitored by a CCD camera (Hamamatsu C 3077) and was either displayed on a computer monitor or stored on a video recorder (Panasonic AG 7350) with the help of a CCD camera control unit (Hamamatsu C 2400) and an image processor (Hamamatsu ARGUS-10). A MacIntosh computer (IIci) was used with the following software: Quick Capture 1.13 (Data Translation, Marlboro, MA, USA), NIH Image 1.43 (Microsoft), and IPLab Spectrum QC (Signal Analytics, Vienna, Austria). Force was monitored with a digital storage oscilloscope (Hitachi VC-6025). For calibration purposes, the force transducer was turned into a vertical position with the connecting tube pointing downwards. Two paper rings of 0.4 mg and 0.76 mg weight were slipped over the wire hook and the deflection of the oscilloscope beam was recorded. Other forces could easily be calculated from the deflection of the oscilloscope beam by using a simple equation.

Cell preparation and solutions

The cell preparation was performed in a Langendorff apparatus as described elsewhere.[16] Briefly, Wistar rats were killed by rapid excision of the heart after anaesthesia. The heart was mounted in the Langendorff apparatus and perfused for 5 min with solution A (mmol/l: NaCl 110; KCl 2.6; KH_2PO_4 1.2; $MgSO_4$ 1.2; HEPES 25; glucose 11; adjusted to pH 7.0 with NaOH). This solution was then replaced by solution B, which was identical to solution A, except that it contained collagenase D (Sigma Chemicals) at a concentration of 166.4 mg/l. Digestion lasted about 20 min. During the final 7 min, calcium (0.2 mmol/l) was added. After digestion the cells were washed and disintegrated in a collagenase-free solution and then skinned in a buffer (mmol/l: EGTA 10; Na_2ATP 3.5) containing 0.5% Triton X-100 for 10 min. This solution was exchanged for relaxing solution (mmol/l: imidazole 30; Na_2ATP 4; creatine phosphate 12; Mg-acetate 3.5; EGTA 10; K-acetate 100.5; leupeptin 0.05), which was used also during measurements of cell length and width. For activation experiments, we used solutions with pCa 7.0, 5.7, 5.46 and 4.9. No activation is expected at pCa 7.0, whereas pCa 4.9 fully activates the contractile apparatus.[3,17] The cells were stored in a buffer containing relaxing solution and glycerol in equal parts.

Experimental protocol

Fifty microlitres of cell suspension were placed on the microscope stage, and cells were selected according to the following criteria:[18,19] rectangular shape with sharp edges, cell length at least 90 μm, and SL at least 1.8 μm. Measurements of cell length,

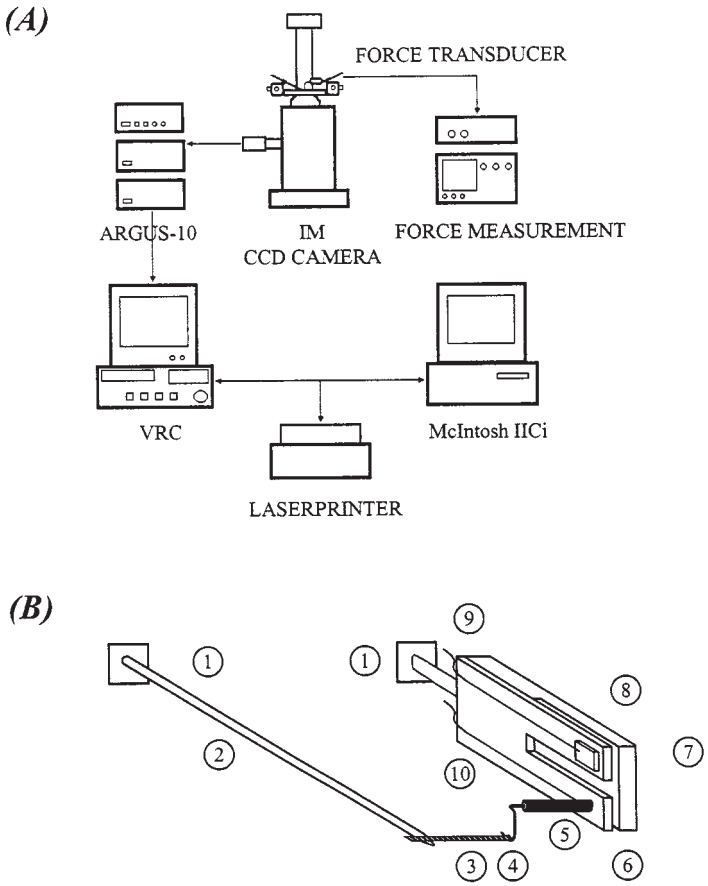

Figure 1 Scheme of experimental setup (A) and transducer system (B). The numbers in (B) indicate: 1 = attachment point to micromanipulator; 2 = glass needle; 3 = myocyte; 4 = wire hook; 5 = connecting tube; 6 = measurement capacitor; 7 = reference capacitor; 8 = compensating mass; 9 and 10 = electrical connections.

cell width, SL and SL inhomogeneity of intact and skinned single myocytes at rest were performed under a 20× objective. For stretch experiments, skinned cells were attached to the glass needle tip and the force transducer with an adhesive containing polyurethane (Great Stuff) and cellulose nitrate (Fig. 2A). Stretch was applied by the micromanipulator-controlled movement of the glass needle with a speed of 5 μm/s.[20,21] Passive force, SL, cell width, and SL inhomogeneity were recorded once a quasi steady-state force level was reached (following $\sim$2 min of stress relaxation). After completion of stress relaxation, cells were activated in solutions of different pCa levels by exchanging the medium three times to replace the relaxing buffer by the activating solution fully. The rise in force was followed on the storage oscilloscope and, after active force reached a constant level, cell images were captured to analyse SL and SL inhomogeneity. Force amplitudes of stretched and calcium-activated cells generally were measured by applying a rapid shortening step to or below slack length.

Measurement of cell dimensions, sarcomere length and sarcomere length inhomogeneity

Calibration of cell length measurement was performed with a gauge beam of known length. SL was measured with two different methods:

(i) The length of a section of about 20 sarcomeres was determined by comparison with the known length of the faded-in gauge-beam and then divided by the number of sarcomeres to obtain the average SL.
(ii) Mean SL was assessed by calculating and inverting the fundamental frequency of the Fourier spectrum (Fig. 2). From the spatial frequency of the sarcomeric pattern, the wavelength was calculated and translated into SL.[15]

SL inhomogeneity corresponds to the FWHM of the first-order peaks (Fig. 2C). Increased SL inhomogeneity leads to a broadening of the first-order line. To avoid an influence of the ROI size on FWHM, we usually selected an area of 512 × 32 pixels,

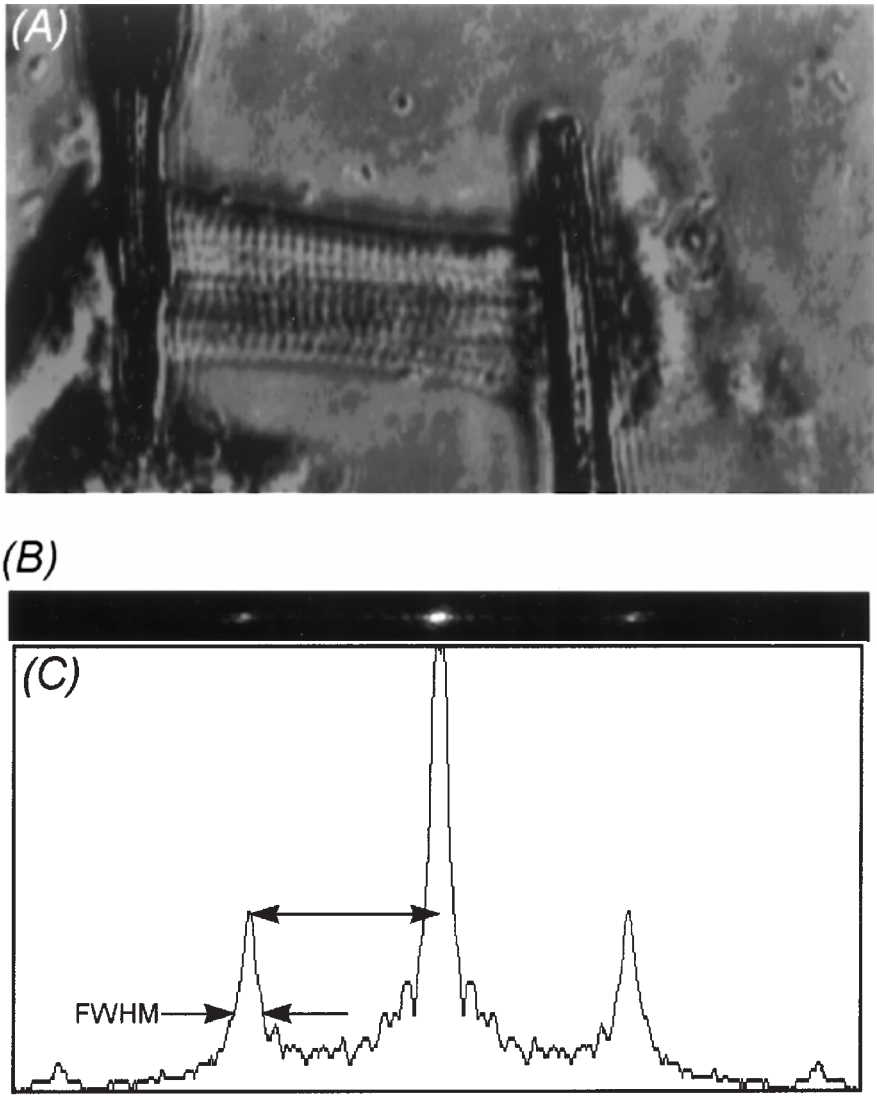

Figure 2 Method of measuring SL and SL inhomogeneity from a cell image. (A) Typical image of a relaxed rat cardiac myocyte suspended at both ends. (B) Two-dimensional FFT spectrum and (C) one-dimensional FFT spectrum, calculated from the spatial frequency of the sarcomeric pattern. Mean SL (here, 2.41 μm) is taken from the fundamental frequency of the FFT spectrum. The full width at half maximum (FWHM) of the first-order peak indicates SL inhomogeneity (here, 0.235 μm).

which fully included the object of interest also at the longest SLs. For analysis, a two-dimensional FFT spectrum was calculated initially (Fig. 2B). The two-dimensional spectrum is sensitive to sarcomere skewing: skewing causes the spectral peaks to be located off the equatorial axis of the spectrum. In the absence of skewing, the peaks are located on the equatorial axis of the spectrum, and both one-dimension and two-dimension based Fourier analyses yield identical results.[15] Therefore, only those experiments were included in the study where spectral peaks were located on the spectrum's equatorial axis—thus indicating no detectable skewing. In such cases the two-dimensional spectrum was collapsed into a one-dimensional spectrum by summing up the pixels perpendicular to the spectrum's equatorial axis (Fig. 2B,C).[15] Another factor to be considered is an "out-of-register" of sarcomeres in the Z-direction. However, the focal depth of the microscope at the magnification chosen was only 5 μm (4–5 myofibrils), and slight misregistration would lead to a decrease in contrast between A- and I-bands, not to a change in apparent SL and SL inhomogeneity.[12] Altogether, the method of detecting SL inhomogeneity by FFT analysis is advantageous when compared with laser dif-

Table 1 Comparison of parameters measured on intact and skinned cardiac cells at slack SL

Parameter	Intact cells	Skinned cells	*P*-value (Student's *t*-test)
Sarcomere length (μm)	1.842 ± 0.078	1.833 ± 0.042	0.49
Cell length (μm)	110.2 ± 10.0	112.3 ± 8.5	0.33
Cell width (μm)	24.6 ± 3.0	25.9 ± 3.4	0.12
Cell length: cell width	4.47	4.35	
FWHM (μm) (inhomogeneity)	0.122 ± 0.039	0.092 ± 0.026	0.0002

Statistically significant differences between both cell types were probed by Student's *t*-test. Most values are given as mean ± S.D.

fractometry,[22] in that it allows a relatively simple experimental setup, the possibility of an exact definition of a region of interest, and low energy exposure of the cell.

Statistics

For most statistical analyses Student's *t*-test was used, either paired or unpaired. Values of $P<0.05$ were regarded as statistically significant.

Single myofibril mechanics

Myofibrils isolated from freshly prepared rat left ventricular tissue were suspended between a micromotor and a sensitive force transducer, and passive length–tension curves were measured as described.[3,21] Relaxing solutions contained, in most cases, the active force-inhibiting drug, 2,3-butanedione monoxime (20 mM), to suppress any contractile activity possibly remaining even in relaxing buffer. In a typical protocol, a single myofibril (or a doublet) was stretched in stages from slack length to a series of desired SLs. Stretch duration was ~20 s; the hold period (to wait for stress relaxation) was 2–3 min. Following stretching to a maximum SL, the specimen was released in stages to slack length. To obtain tension, the cross-sectional area of a preparation was inferred from the specimen's diameter as described.[21]

Results

Mechanical properties of non-activated cells

A total of 113 cells were included in the analysis: 30 intact and 83 skinned cells. Table 1 shows data of skinned and intact myocytes at rest. Cellular dimensions and slack SLs were similar to values reported elsewhere[6,18,23] and were comparable in intact and skinned myocytes. However, a statistically significant difference was found for FWHM (SL inhomogeneity), which was lower in skinned myocytes than in intact cells ($P<0.001$).

A typical force response of a skinned cardiomyocyte stretched with constant speed to near 2.6 μm SL is shown in Figure 3A (inset). At quasi-steady state, force reached a value of ~1 mg. To relate the measured force to the tension, a cell's cross-sectional area is required. We calculated the cross-sectional area from the cell width. Based on three-dimensional (3D) reconstructions of optical sections of rat cardiac myocytes (obtained by laser-scanning microscopy; data not shown), we assumed an oval cross-sectional area with a constant width: thickness ratio of 1.67:1, which is thought to be stretch-independent.[17,20] Steady-state tension in the example of Figure 3A (inset) was 32 mN/mm^2. Results of such kinds of experiments are summarized in Figure 3A; tension, σ, was plotted against SL, and data were fitted by the equation:

$$\sigma = 4.413*[\exp(2.873*(SL-1.845))-1];\ r^2 = 0.92. \quad (1)$$

The passive length–tension curve was comparable to that described by others for skinned rat cardiac cells.[4,24]

We also investigated the relationship between SL and FWHM (SL inhomogeneity) upon cell stretch. Figure 3B shows that FWHM increased with SL. The data was fitted by a simple:

$$FWHM = 0.326*SL-0.436;\ r^2 = 0.83. \quad (2)$$

In addition, we compared the SL inhomogeneity near the cell attachment sites to that of the middle portion of the myocyte. No statistically significant difference was found, either in cells at slack length or in cells stretched to ~2.5 μm SL (data not shown).

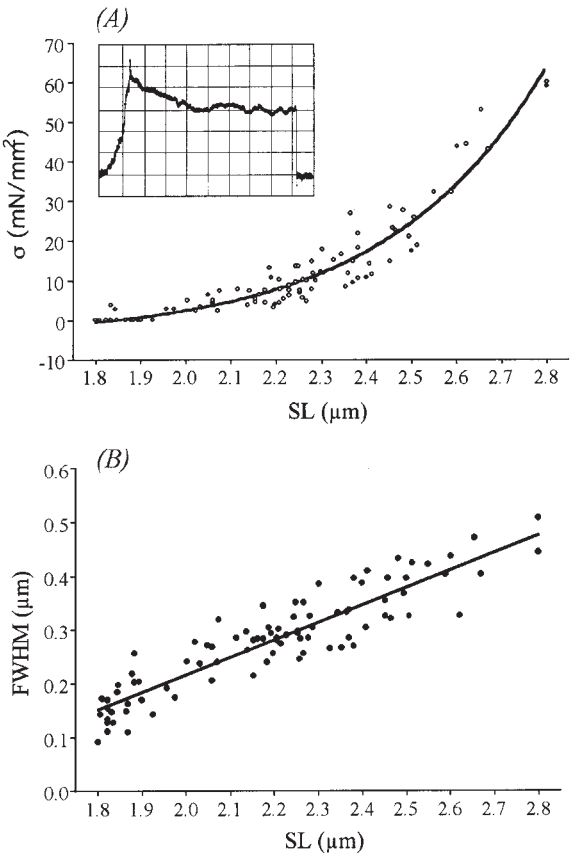

Figure 3 Passive tension and SL inhomogeneity upon stretch of skinned rat cardiac cells. (A) SL-tension relation in relaxing buffer. Data points were fitted with Eqn (1). Inset: representative force trace recorded during a stretch-hold protocol. After the stretching stopped, force decayed to a quasi-steady state level whose magnitude was measured by quickly releasing the cell to slack SL. Increment on abscissa equals 20 s, on ordinate 50 mV (0.37 mg). (B) Dependence of FWHM on SL. Data were fitted with Eqn (2). ROIs: 512×32 pixels.

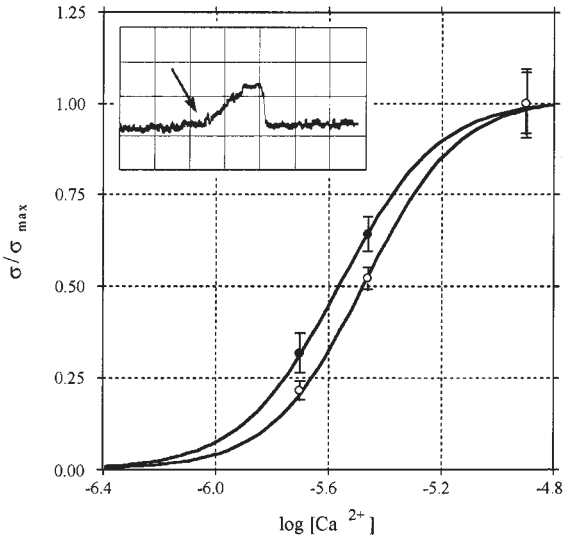

Figure 4 Relative tension *v* log $[Ca^{2+}]$, measured in skinned cardiac cells. Data are shown as mean $\pm$ SD and fitted using the Hill equation [Eqn (3)]. Filled circles: tension at SL $= 2.20 \pm 0.04$ μm (mean $\pm$ SD, $n = 6$), HC $=$ 2.484, $K_c = 1.585*10^{-14}$. Open circles: tension at SL $=$ 1.87 ± 0.02 μm (mean $\pm$ SD, $n = 4$), HC $= 2.613$, $K_c =$ $5.012*10^{-15}$. Curve shift at $\sigma/\sigma_{max} = 0.5$ is 0.1 pCa units. Inset: original force trace recorded during activation of a skinned cardiac cell with pCa 5.46 solution (SL $=$ 1.90 μm). The time of application of Ca^{2+}-containing buffer is indicated by the arrow. Note that force rises to a plateau level, before the cell is returned quickly to below slack SL. Increment on abscissa equals 20 s, on ordinate 50 mV (0.37 mg).

Calcium sensitivity of rat cardiac cells and active length–tension relation

To determine the calcium concentration necessary for full activation, active tension generation was investigated in bathing solutions containing different $[Ca^{2+}]$. An original force trace is shown in the inset of Figure 4; a skinned myocyte was activated at 1.9 μm SL in pCa 5.46 solution. Active force rose to a constant maximum level (0.43 mg), before the cell was quickly released to below slack length. The main Figure 4 demonstrates that full activation was reached near pCa 4.9. Because the SL affects the calcium sensitivity of myofilaments, tension was measured at two different degrees of stretching, 2.20 ± 0.04 μm (mean $\pm$ SD, $n = 6$) and 1.87 ± 0.02 μm SL ($n = 4$), respectively. Figure 4 shows the two curves calculated from data points of relative tension, σ/σ_{max} *v* log$[Ca^{2+}]$ according to the Hill equation:

$$\sigma = \sigma_{max} * [Ca^{2+}]^{HC}/(K_c + [Ca^{2+}]^{HC}) \qquad (3)$$

where HC (the Hill coefficient) and K_c are constants. The results confirmed the expected change in calcium sensitivity of the contractile machinery: upon increasing the SL by ~ 0.3 μm, the curve shifted leftward by 0.1 pCa units at $\sigma = 0.5\ \sigma_{max}$. The Hill coefficient adopted values of 2.48 (SL $= 2.20$ μm) and 2.61 (SL $= 1.87$ μm)—well within the range known for skinned cardiac preparations.[17,25] Thus, the cells used in this study exhibit normal contractile properties.

Active tension was measured altogether in 37 skinned cardiac cells and was calculated by subtracting passive from total tension. Maximum active tension levels (60–70 mN/mm^2) reached the typical values found in skinned cardiac specimens.[9,26] SL was determined from the FFT spectra recorded during active force development. Figure 5 summarizes the active length–tension relations obtained

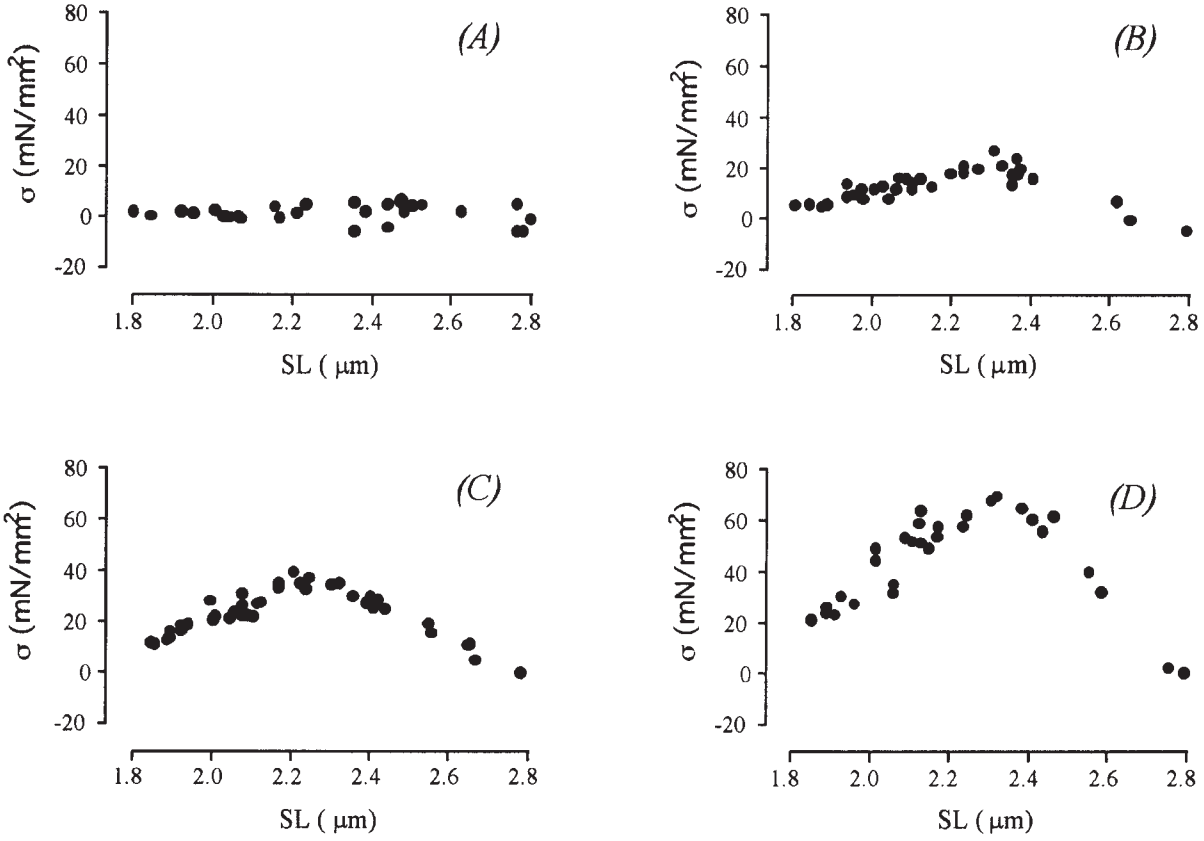

Figure 5 Active length–tension relations of skinned cardiac cells activated in solutions containing different Ca^{2+} levels: (A) pCa 7.0; (B) pCa 5.7; (C) pCa 5.46, (D) pCa 4.9. Each plot contains data obtained from 10 different cells. Note the local force maximum between 2.2 and 2.4 μm SL and zero force generation of cells activated at $\sim$2.8 μm SL.

at pCa 7.0 (A), 5.7 (B), 5.46 (C), and 4.9 (D); an SL range from 1.8 μm to almost 3.0 μm was investigated. In (B), (C), and (D), a local tension maximum is seen between 2.2 and 2.4 μm SL. The myocytes could readily be stretched up to the point where active tension development reached zero: tension became undetectable near 2.8 μm SL.

SL and SL inhomogeneity during calcium activation

The effect of calcium activation on SL inhomogeneity was tested in skinned cardiac cells at SLs between 1.8 and $\sim$2.8 μm. Results are shown in Figure 6: mean SLs and FWHM are plotted as the ratio of post-activation value:pre-activation value *vs* SL. Pre-activation levels are considered to be 100%. The analysis was made again at four different pCa levels, pCa 7.0 [Fig. 6 (A), pCa 5.7 (B), pCa 5.46 (C), and pCa 4.9 (D)]. Figure 6 indicates a small decrease of relative SL (open squares) during activation, presumably due to the compliance of the force transducer. On the other hand, SL-inhomogeneity (filled squares) increased upon activation, depending on calcium concentration. Possible artifacts due to solution exchange did not appear to affect the results, since at pCa 7.0 no change of mean SL and SL inhomogeneity was detectable. To check for possible variability in SL distribution along the activated cell, myocytes were "virtually" subdivided into three equal partitions, a middle region and both end regions. The mean SL was measured in each partition (Table 2). These measurements were made at high Ca^{2+} activation levels and at SLs of $\sim$2.2 and $\sim$2.7 μm, respectively. Table 2 demonstrates that neither a statistically significant difference of mean SL, nor differences in the standard deviations, were found among the three partitions. Thus, substantial variability in SL distribution along a highly stretched cell during activation could be excluded. This finding was further supported by the results of the FWHM analysis (Fig. 6): at long SLs

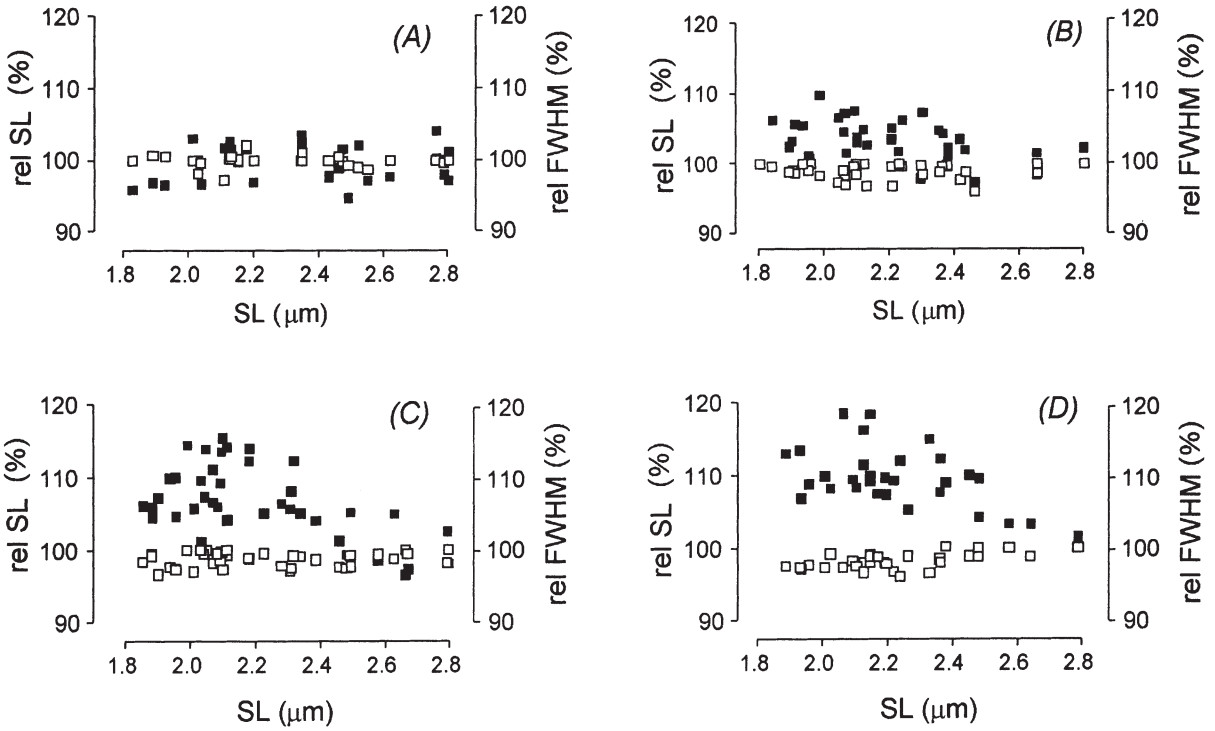

Figure 6 Change of SL and SL inhomogeneity during cell-isometric contraction in solutions containing different Ca^{2+} levels: (A) pCa 7.0; (B) pCa 5.7; (C) pCa 5.46, (D) pCa 4.9. Relative SL (open squares) and relative FWHM (filled squares) are shown as the ratio post-activation value:pre-activation value *v* SL before activation. Note in (B), (C) and (D) a small decrease of relative SL and a substantial rise of SL inhomogeneity (relative FWHM) with increasing level of activation. At long SLs, however, FWHM remained almost unchanged upon activation.

Table 2 Sarcomere lengths and standard deviations of stretched skinned cells during activation

	Shorter cells ($n=8$)	Longer cells ($n=11$)
Average mean SL (μm)	2.186 ± 0.055	2.683 ± 0.104
Mean SL of F (μm)	2.176 ± 0.064	2.679 ± 0.126
Mean SL of M (μm)	2.201 ± 0.057	2.683 ± 0.137
Mean SL of N (μm)	2.180 ± 0.069	2.686 ± 0.102

For analysis, the myocytes were subdivided into three equal partitions, one at the force transducer end (F), a second in the middle region (M), and a third near the needle attachment site (N). For comparison, average mean SL ± S.D. is also shown. Cells activated at pCa 4.9 or pCa 5.46 and at SLs of ~2.2 and ~2.7 μm were examined. A statistically significant difference (measured by Student's *t*-test) between partitions was not found.

(>2.5 μm), the increase in SL inhomogeneity upon activation was usually much smaller than that observed at shorter SLs.

Finally, we used linear regression (least-squares method) to test whether or not the active force level depended on SL inhomogeneity, but found no statistically significant dependence (data not shown).

Force-bearing capacity of single cardiac myofibrils

In search of an explanation for the relatively short descending limb of the active SL–tension relation, the extension properties of cardiac cells were investigated at the level of the sarcomere. To this end, single rat cardiac myofibrils were stretched under relaxing conditions in a setup described previously[3,21] and passive force was measured. Most likely, the force is developed by the elastic section of titin filaments, the giant proteins of the sarcomere.[3,4,21] Figure 7 shows the myofibrillar force response to imposed stretches up to ~3.4 μm SL. When the data of many measurements were pooled (main Fig. 7), it appeared that between 1.8 and 2.8 μm SL, the shape of the passive tension curve of single myofibrils, was more or less similar to that of single cells (Fig. 3A) and exhibited a quasi-exponential rise. As shown in Figure 7, passive tension of single myofibrils began to increase less

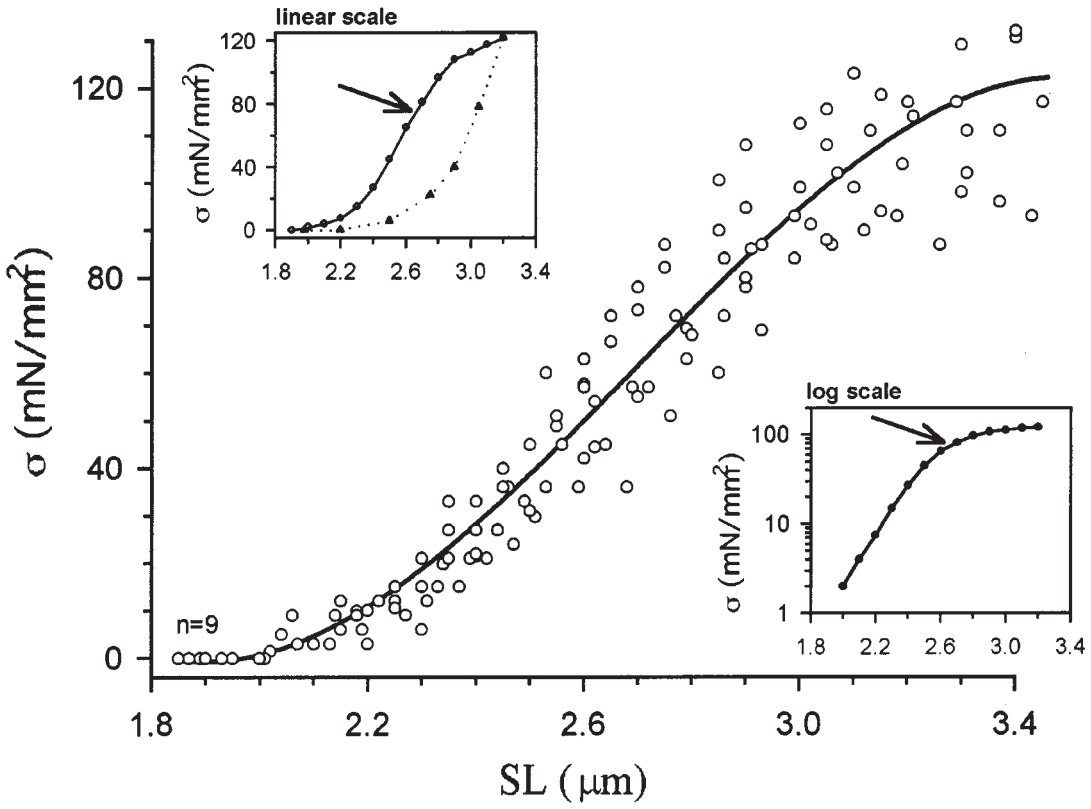

Figure 7 Passive length–tension relations of single rat cardiac myofibrils. Data were pooled and fitted by third-order regression. Inset in upper left-hand corner: passive tension recorded in a typical experiment during stretching (continuous line) and release (broken line) of a single myofibril. Note a first decrease in the slope of the stretch curve (arrow) at 2.6–2.7 μm SL and a flattening of the curve at 2.8–3.0 μm SL. The release curve lies much below the stretch curve, indicating large hysteresis. After stretch to 3.2 μm SL, the myofibril fails to return to its initial slack SL. Inset in lower left-hand corner: same experiment, but plot of log force during stretch *v* SL. The first slope change at 2.6–2.7 μm SL (arrow) becomes more clearly detectable.

steeply above 2.8 μm SL. Some interesting additional features in the high-extension regime were revealed upon analysis of individual experiments. Such experiments demonstrated a first decrease in the slope of the passive tension curve between 2.6 and 2.7 μm SL (inset in upper left-hand corner of Fig. 7). This deviation from the quasi-exponential force rise becomes more clearly detectable when log force is plotted against SL (inset in lower right-hand corner of Fig. 7). Between 2.8 and 3.0 μm SL the curve flattens further, which may indicate the reach of a "strain limit". The strain limit SL has been shown to correlate with the onset of severe structural changes within the sarcomere, most notably thick-filament disarray and disruption of the composite thick filament made up of myosin and titin.[24,27,28] Irreversible structural alterations could indeed be inferred from our observation that the release curve after high stretching was generally much below the stretch curve (indicating large hysteresis) and did not return to the initial slack-SL value (inset in upper left-hand corner of Fig. 7). We then suggest that the structural changes associated with high stretching may strongly impair the ability of myosin to interact with thin filaments and generate active force. This may result in the observed steep decrease in active tension of cardiac sarcomeres approaching a length of 2.8–3.0 μm.

Discussion

In this study, a FFT method was employed to evaluate SL and SL inhomogeneity during stretching and active contraction of single skinned rat cardiac cells. The approach is based on previous reports demonstrating that computer-aided analysis of the intensity profiles recorded from cellular regions represents a precise means of measuring SL and SL inhomogeneity in single-cell preparations,[12,13] particularly when

coupled with FFT.[14,15] A main focus of the present analysis was to investigate SL inhomogeneity of cells over a wide range of SL.

Examination of non-activated myocytes at rest revealed that more or less all cells exhibit some SL inhomogeneity. This finding is perhaps attributable to the "field structure" of a cardiac myocyte[29] consisting of domains within which SLs are closely coupled; SL variability is found mainly between domains.[29] Also, SL inhomogeneity was lower in skinned than in intact cells, consistent with an earlier report.[9] This might be related to optical distortion by nuclei, mitochondria, and sarcoplasmic reticulum,[13,30] structures which are eliminated during chemical skinning. Another factor could be spontaneous Ca^{2+} oscillations even in diastole leading to microscopic, spontaneous, contractile activity and SL inhomogeneity.[16,31,32] Removal or functional inactivation of the calcium-sensitive structures may reduce the inhomogeneity.

Upon stretching of non-activated cardiac cells, SL inhomogeneity increases,[2,19] as confirmed in the present study (Fig. 3). We found that this phenomenon was not due to a different stretching behavior of sarcomeres in the middle of the cell and of those near the cell-attachment sites. SL inhomogeneity was also unlikely to arise from asymmetric glueing, because care was taken to exclude skewed cells from the analysis. The most likely explanation for the stretch-induced increase in SL inhomogeneity may be sought in the above-mentioned sarcomeric field structure:[29] a slightly different response of neighboring domains to stress might lead to increased SL inhomogeneity. Support for this idea comes from the finding that in relaxed single cardiac myofibrils, which of course lack such domains, SLs are more uniform during stretching.[3] In summary, increased SL inhomogeneity after stretching may arise primarily from a different stress response of loosely coupled domains within a cardiac cell.

A chief goal of this study was the analysis of SL and SL inhomogeneity during active force development at different degrees of cell stretching. Since *in vivo* cardiac muscle operates at relatively short SLs compared to skeletal muscles, the cardiac length–tension relation has been studied mainly in the normal working range of ~ 1.7 to ~ 2.3 μm SL.[1] On the other hand, some regions of the heart may be stretched to beyond these SLs under certain pathological conditions, as in dilated cardiomyopathy or end-stage heart failure. Therefore, it is of interest to study how active force generation changes on high sarcomere extension. A difficulty is that continuous stretching of "standard" cardiac specimens (papillary muscles and trabeculae) does not result in a linear increase in mean SL. Even at high stretch forces, mean SL usually does not exceed ~ 2.4 μm, because damage of glued/clipped end regions leads to a high compliance of these regions.[33,34] Moreover, during activation, substantial internal sarcomere shortening is observed.[7,35] The lack of homogeneous activation has prevented faithful measurements of the length–tension curve in larger cardiac specimens. With the advent of the single-cell preparation, [6] more homogeneous activations were achieved.[23] However, attempts to determine the full-range SL–active tension relation have been infrequent and somewhat inconclusive. We know of no study in which a complete descending limb of the cardiac length–tension curve was obtained.

In the present study, we succeeded in measuring active forces of single rat cardiomyocytes over a wide length range. At both submaximal (pCa 5.7, pCa 5.46) and full (pCa 4.9) activation, a local maximum was observed in the active length–tension curve near 2.3 μm SL—a value similar to that found in the literature.[1] Although at submaximal calcium activation the tension level of cardiac cells of some species (for example, dog) can apparently increase even above 2.4 μm SL, this may not be the case in the rat muscle used here.[10] A striking observation made by us was that in rat cardiomyocytes activated at longer SLs, force dropped to zero already at ~ 2.8 μm (Fig. 5). Interestingly, comparison with a previous study by Fabiato and Fabiato[10] reveals remarkable similarities: the authors followed the descending limb of rat cardiac cells up to the point where force dropped to 50% of maximum force at pCa 5.0. By extrapolating their force curve down to SL axis at zero force, we find the point of interception also to be below 3.0 μm. On the other hand, we showed by monitoring SL distribution and FWHM during activation that this short descending limb is unlikely to be due to increased SL inhomogeneity. Hence, the early drop in active force may be a genuine property of the cardiac sarcomere.

These observations imply that the descending limb of the cardiac length–tension relation may not be determined solely by the degree of actin–myosin overlap; additional phenomena may be important. The issue was addressed in mechanical studies on single cardiac myofibrils (Fig. 7), and an involvement of titin filaments was suggested. We first remember that these filaments span half-sarcomeres from the Z-line to the M-line, but are elastic only in the I-band.[36,37] In cardiac muscle, I-band titin is relatively short, whereas skeletal muscles express much longer I-band titins.[21,38] We propose that the tissue type-dependent expression of titin isoforms could lead to variations in the descending limb of the length–

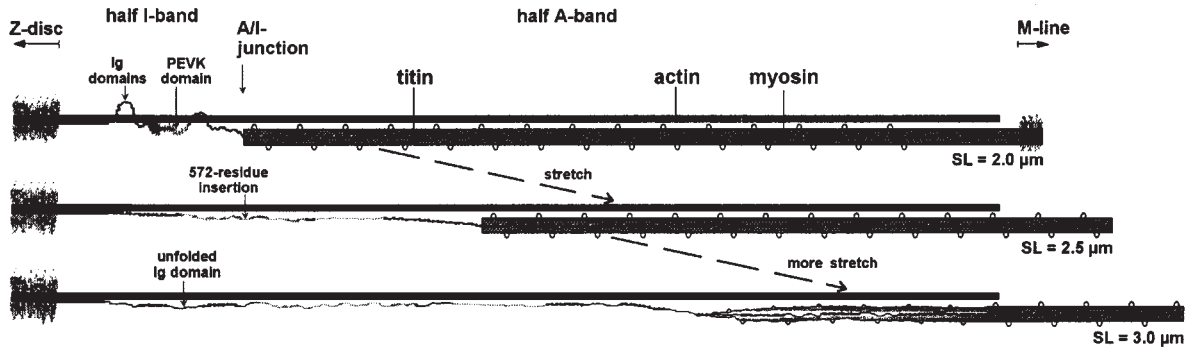

Figure 8 Model of the three filament systems in a (half-)sarcomere and structural changes occurring on high stretch. Overlap between actin and myosin filaments decreases with stretch to above ~2.2 μm SL. Titin filaments, which span from the Z-disk to the M-line, are bound to thick-filament proteins in the A-band but are elastic in the I-band. In cardiac muscle, the elastic titin section (N2-B titin isoform) consists of three extensible elements: stretches of Ig-like globular domains, the PEVK domain, and a 572-residue unique sequence insertion.[38,41] On stretching to above 2.5–2.6 μm SL, titin Ig domains may begin to unfold irreversibly. Near 2.8 μm SL, thick-filament disarray may occur and A-band ends may become disrupted, presumably mediated by unfolding of the globular titin domains normally bound to myosin.

tension relation. How then would titin filaments, which are not directly involved in the process of active force generation, affect the shape of the length–tension curve?

To answer this question, some structural and functional properties of titin must be recalled. The giant titin polypeptide consists of many repeating modules, fibronectin type-III-like and immunoglobulin-like (Ig) domains.[38] These domains bind to thick-filament proteins, such as myosin, which renders A-band titin functionally stiff under normal conditions.[24,39] The I-band portion of titin provides the sarcomere with elasticity.[40] The extensible titin section comprises structurally distinct elements, unique intervening sequences flanked by Ig-domain regions whose modules adopt a β-sheet fold (Fig. 8).[36,38,41] During physiological stretching of cardiac sarcomeres (<2.4 μm SL), the Ig domains remain folded,[41,42] but modules may unfold irreversibly on stretching to above 2.5–2.6 μm SL.[41] Unfolding would be predicted to result in a change in the slope of the SL-passive force curve, just as found in single cardiac myofibrils stretched to above 2.6–2.7 μm (Fig. 7).

Ig-domain unfolding may have dramatic effects on sarcomeric organization. Most importantly, it may trigger progressive detachment of titin from the thick filament—a process for which ultrastructural evidence was provided.[24,28] The detachment most likely explains why the slope of the passive length–tension curve of cardiac myofibrils becomes greatly reduced at 2.8–3.0 μm SL (Fig. 7). Figure 8 schematically demonstrates our view of how extreme stretch leads to a disruption of thick-filament ends. Also, when passive force levels are greatly increased at very long SLs, thick filaments may become misaligned, as demonstrated by electron microscopy of highly stretched rat cardiac sarcomeres.[24] Clearly, thick-filament disarray and disruption of A-band ends will affect active force. Taken together, we argue that, beginning at SLs much below 3 μm in rat cardiac cells, the ability of myosin to generate active force is impaired by severe structural damage. Consequently, the descending limb of the active length–tension curve will be abbreviated. Finally, the expression of different length isoforms of titin in skeletal and cardiac muscle[38] may explain why the descending limb has a different shape in the two muscle types: unfolding of Ig domains and disruption of the titin–thick-filament complex will begin at much longer SLs in skeletal muscles (above 3.6 μm)[27,28] than in the heart.

To sum up, stretching of rat cardiac sarcomeres to lengths above 2.6–2.8 μm may trigger irreversible structural alterations within I-band titin and the titin–thick-filament complex, accompanied by impairment of active force generation. Thus, the descending limb of the cardiac length–tension curve may be determined only in part by the degree of actin–myosin overlap; the intrinsic properties of titin filaments may be equally important.

Acknowledgments

The authors would like to thank J. C. Rüegg and H. Granzier for support at the early stages of this study. We also thank S. Schmerling for help with the FFT evaluation method and S. Boldt for excellent technical assistance. Financial support of the

Deutsche Forschungsgemeinschaft is greatly acknowledged (Li 690/2-2, SFB 320 to WAL).

References

1. Allen DG, Kentish JC. The cellular basis of the length–tension relation in cardiac muscle. *J Mol Cell Cardiol* 1985; **17**: 821–840.
2. Brady AJ. Mechanical properties of isolated cardiac myocytes. *Physiol Rev* 1991; **71**: 413–428.
3. Linke WA, Popov VI, Pollack GH. Passive and active tension in single cardiac myofibrils. *Biophys J* 1994; **67**: 782–792.
4. Granzier HL, Irving TC. Passive tension in cardiac muscle: Contribution of collagen, titin, microtubules, and intermediate filaments. *Biophys J* 1995; **68**: 1027–1044.
5. Pollack GH, Huntsman LL. Sarcomere length-active force relations in living mammalian cardiac muscle. *Am J Physiol* 1974; **227**: 383–389.
6. Fabiato A, Fabiato F. Dependence of the contractile activation of skinned cardiac cells on the sarcomere length. *Nature* 1975; **256**: 54–56.
7. Julian FJ, Sollins MR. Sarcomere length–tension relations in living rat papillary muscle. *Circ Res* 1975; **37**: 299–308.
8. Ter Keurs HEDJ, Rijnsburger WH, Van Heuningen R, Nagelsmit MJ. Tension development and sarcomere length in rat cardiac trabeculae. *Circ Res* 1980; **46**: 703–714.
9. Kentish JC, ter Keurs HE, Ricciardi L, Bucx JJ, Noble MI. Comparison between the sarcomere length-force relations of intact and skinned trabeculae from rat right ventricle. Influence of calcium concentrations on these relations. *Circ Res* 1986; **58**: 755–768.
10. Fabiato A, Fabiato F. Myofilament-generated tension oscillations during partial calcium activation and activation dependence of the sarcomere length–tension relation of skinned cardiac cells. *J Gen Physiol* 1978; **72**: 667–699.
11. Gordon AM, Huxley AF, Julian FJ. The variation in isometric tension with sarcomere length in vertebrate muscle fibres. *J Physiol (Lond)* 1966; **184**: 170–192.
12. Roos KP, Brady AJ, Tan T. Direct measurement of sarcomere length from isolated cardiac cells. *Am J Physiol* 1982; **242**: H68–H78.
13. Roos KP. Sarcomere length uniformity determined from the three-dimensional reconstruction of resting isolated heart cell striation patterns. *Biophys J* 1987; **52**: 317–327.
14. Gannier F, Bernengo JC, Jacquemond V, Garnier D. Measurements of sarcomere dynamics simultaneously with auxotonic force in isolated cardiac cells. *IEEE Trans Biomed Eng* 1993; **40**: 1226–1232.
15. Slawnych MP, Morishita L, Bressler BH. Spectral analysis of muscle fiber images as a means of assessing sarcomere heterogeneity. *Biophys J* 1996; **70**: 38–47.
16. Wussling MHP, Salz H. Nonlinear propagation of spherical calcium waves in rat cardiac myocytes. *Biophys J* 1996; **70**: 1144–1153.
17. Fabiato A. Myoplasmic free calcium concentration reached during the twitch of an intact isolated cardiac cell and during calcium-induced release of calcium from the sarcoplasmic reticulum of a skinned cardiac cell from the adult rat or rabbit ventricle. *J Gen Physiol* 1981; **78**: 457–497.
18. Roos KP, Brady AJ. Individual sarcomere length determination from isolated cardiac cells using high-resolution optical microscopy and digital image processing. *Biophys J* 1982; **40**: 233–244.
19. Palmer RE, Brady AJ, Roos KP. Mechanical measurements from isolated cardiac myocytes using a pipette attachment system. *Am J Physiol* 1996; **270**: C697–C704.
20. Brady AJ. Length dependence of passive stiffness in single cardiac myocytes. *Am J Physiol* 1991; **260**: H1062–H1071.
21. Linke WA, Ivemeyer M, Olivieri N, Kolmerer B, Rüegg JC, Labeit S. Towards a molecular understanding of the elasticity of titin. *J Mol Biol* 1996; **261**: 62–71.
22. Wussling MHP, Schenk W, Nilius B. A study of dynamic properties in isolated myocardial cells by the laser diffraction method. *J Mol Cell Cardiol* 1987; **19**: 897–907.
23. Krueger JW, Forletti D, Wittenberg BA. Uniform sarcomere shortening behavior in isolated cardiac muscle cells. *J Gen Physiol* 1980; **76**: 587–607.
24. Trombitas K, Jin J-P, Granzier H. The mechanically active domain of titin in cardiac muscle. *Circ Res* 1995; **77**: 856–861.
25. Kentish JC. The inhibitory effect of monovalent ions on force development in detergent-skinned ventricular muscle from guinea-pig. *J Physiol* 1984; **352**: 353–374.
26. Stienen GJM, Papp Z, Elzinga G. Calcium modulates the influence of length changes on the myofibrillar adenosine triphosphate activity in rat skinned cardiac trabeculae. *Pflügers Arch* 1993; **425**: 199–207.
27. Wang K, McCarter R, Wright J, Beverly J, Ramirez-Mitchell R. Regulation of skeletal muscle stiffness and elasticity by titin isoforms: A test of the segmental extension model of resting tension. *Proc Natl Acad Sci USA* 1991; **88**: 7101–7105.
28. Wang K, McCarter R, Wright J, Beverly J, Ramirez-Mitchell R. Viscoelasticity of the sarcomere matrix of skeletal muscles. The titin-myosin composite filament is a dual-stage molecular spring. *Biophys J* 1993; **64**: 1161–1177.
29. Palmer RE, Roos KP. Extent of radial sarcomere coupling revealed in passively stretched cardiac myocytes. *Cell Motil Cytoskeleton* 1997; **37**: 378–388.
30. Cheung JY, Tillotson DL, Yelamarty RV, Scaduto Jr RC. Cytosolic free calcium concentration in individual cardiac myocytes in primary culture. *Am J Physiol* 1989; **256**: C1120–C1130.
31. Lakatta EG, Talo A, Capogrossi MC, Spurgeon HA, Stern MD. Spontaneous sarcoplasmic reticulum Ca^{2+} release leads to heterogeneity of contractile and electrical properties of the heart. *Basic Res Cardiol* 1992; **87** (Suppl. 2): 93–104.
32. Tanaka H, Sekine T, Kawanishi T, Nakamura R, Shigenobu K. Intrasarcomere $[Ca^{2+}]$ gradients and their spatio-temporal relation to Ca^{2+} sparks in rat cardiomyocytes. *J Physiol (Lond)* 1998; **508**: 145–152.
33. Huntsman LL, Day SR, Stewart DK. Nonuniform

contraction in the isolated cat papillary muscle. *Am J Physiol* 1977; **233**: H613–H616.
34. Donald TC, Reeves DNS, Reeves RC, Walker AA, Hefner LL. Effect of damaged ends in papillary muscle preparations. *Am J Physiol* 1980; **238**: H14–H23.
35. Krueger JW, Pollack GH. Myocardial sarcomere dynamics during isometric contraction. *J Physiol (Lond)* 1975; **251**: 627–643.
36. Labeit S, Kolmerer B, Linke WA. The giant protein titin. Emerging roles in physiology and pathophysiology. *Circ Res* 1997; **80**: 290–294.
37. Gregorio CC, Granzier H, Sorimachi H, Labeit S. Muscle assembly: a titanic achievement? *Curr Opin Cell Biol* 1999; **11**: 18–25.
38. Labeit S, Kolmerer B. Titins, giant proteins in charge of muscle ultrastructure and elasticity. *Science* 1995; **270**: 293–296.
39. Fürst DO, Osborn M, Nave R, Weber K. The organization of titin filaments in the half-sarcomere revealed by monoclonal antibodies in immunoelectron microscopy: a map of ten nonrepetitive epitopes starting at the Z-line extends close to the M-line. *J Cell Biol* 1988; **106**: 1563–1572.
40. Linke WA, Granzier H. A spring tale: New facts on titin elasticity. *Biophys J* 1998; **75**: 2613–2614.
41. Linke WA, Rudy DE, Centner T, Gautel M, Witt C, Labeit S, Gregorio CC. I-band titin in cardiac muscle is a three-element molecular spring and is critical for maintaining thin filament structure. *J Cell Biol* 1999; **146**: 631–644.
42. Helmes M, Trombitas K, Centner T, Kellermayer M, Labeit S, Linke WA, Granzier H. Mechanically driven contour-length adjustment in rat cardiac titin's elastic segment: N2B cardiac titin is an adjustable spring. *Circ Res* 1999; **84**: 1339–1352.